

PCCP

Accepted Manuscript



This is an *Accepted Manuscript*, which has been through the Royal Society of Chemistry peer review process and has been accepted for publication.

Accepted Manuscripts are published online shortly after acceptance, before technical editing, formatting and proof reading. Using this free service, authors can make their results available to the community, in citable form, before we publish the edited article. We will replace this *Accepted Manuscript* with the edited and formatted *Advance Article* as soon as it is available.

You can find more information about *Accepted Manuscripts* in the [Information for Authors](#).

Please note that technical editing may introduce minor changes to the text and/or graphics, which may alter content. The journal's standard [Terms & Conditions](#) and the [Ethical guidelines](#) still apply. In no event shall the Royal Society of Chemistry be held responsible for any errors or omissions in this *Accepted Manuscript* or any consequences arising from the use of any information it contains.

PCCP Guidelines for Referees

Physical Chemistry Chemical Physics (PCCP) is a high quality journal with a large international readership from many communities

Only very important, insightful and high-quality work should be recommended for publication in PCCP.



To be accepted in PCCP - a manuscript must report:

- Very high quality, reproducible new work
- **Important new physical insights** of significant general interest
- A novel, stand-alone contribution

Routine or incremental work should not be recommended for publication. Purely synthetic work is not suitable for PCCP

If you rate the article as 'routine' yet recommend acceptance, please give specific reasons in your report.

Less than 50% of articles sent for peer review are recommended for publication in PCCP. The current PCCP Impact Factor is 3.83

PCCP is proud to be a leading journal. We thank you very much for your help in evaluating this manuscript. Your advice as a referee is greatly appreciated.

With our best wishes,

Philip Earis (pccp@rsc.org)
Managing Editor, PCCP

Prof Daniella Goldfarb
Chair, PCCP Editorial Board

General Guidance (For further details, see the RSC's [Refereeing Procedure and Policy](#))

Referees have the responsibility to treat the manuscript as confidential. Please be aware of our [Ethical Guidelines](#) which contain full information on the responsibilities of referees and authors.

When preparing your report, please:

- Comment on the originality, importance, impact and scientific reliability of the work;
- State clearly whether you would like to see the paper accepted or rejected and give detailed comments (with references) that will both help the Editor to make a decision on the paper and the authors to improve it;

Please inform the Editor if:

- There is a conflict of interest;
- There is a significant part of the work which you cannot referee with confidence;
- If the work, or a significant part of the work, has previously been published, including online publication, or if the work represents part of an unduly fragmented investigation.

When submitting your report, please:

- Provide your report rapidly and within the specified deadline, or inform the Editor immediately if you cannot do so.
- We welcome suggestions of alternative referees.

Plasmonic rod-in-shell nanoparticles for photothermal therapy

Cite this: DOI: 10.1039/x0xx00000x

Shanshan Wang, Hong Xu* and Jian Ye*

Received 00th January 2012,
Accepted 00th January 2012

DOI: 10.1039/x0xx00000x

www.rsc.org/

The plasmonic gold nanoparticles are promising candidates for photothermal therapy (PTT) application. The optical properties of various gold nanoparticles have been widely investigated for PTT application in the first near-infrared (NIR) window (650 – 950 nm). However, few studies are reported about the nanoparticles employed in the second NIR window (1000 – 1350 nm) where light penetrates through the tissue deeper. Recently a new type of plasmonic rod-in-shell (RIS) nanoparticles that can be optically responsive in the second NIR window has been reported (*ACS Nano*, 2013, 7, 5330). In this article, we employed an extensive numerical exploration of the optical absorption properties of the RIS particles by tuning their dimensional parameters including the core length, gap size and shell thickness. A number of favorable optical properties of the RIS nanoparticle potentially for the better PTT effect have been observed including: (1) the strong and highly tunable optical absorption in the second NIR window with a particle size less than 100 nm; (2) a larger absorption cross-section both in the first and second NIR window over a nanorod with the same gold mass; and (3) particles' orientation insensitive light absorption in the first NIR window due to the overlapping of the longitudinal and transverse mode. These unique optical properties imply the RIS nanoparticle could become a promising candidate for the PTT application in the first and second NIR window.

Introduction

Plasmonic photothermal therapy (PTT) is a novel and promising method in cancer therapy that utilizes selective laser light and employs metallic photothermal nanoparticles that can target the tumor cells. The incident laser excites the localized surface plasmon resonance (LSPR) on the nanoparticles that converts light into heat and causes irreversible damage to the tumor tissues without hurting the healthy tissues. Compared with traditional cancer therapy methods like surgery and chemotherapy, it is minimally-invasive to the healthy tissues¹. The utilization of metallic plasmonic nanoparticles in PTT has been widely investigated over the past few years.^{2,3} It has been found that the light absorption cross section of the metallic nanoparticles can have four to five orders of magnitude greater than that of the conventional photoabsorbing dyes.^{4,5} The gold nanoparticles are promising candidates for the application of PTT because their surface is easier to be functionalized with the ligands targeted to the tumor cells using the Au-S bond. In addition, they have good biocompatibility for the possible *in vivo* long-term circulations.⁶⁻⁹ The preferred size of the gold nanoparticles should be less than 100 nm, because larger gold nanoparticles show a shorter circulating half-life and are more rapidly cleared by the reticuloendothelial system (RES), which is not favourable for the specific targeting to the tumor sites during the treatment.^{10,11} Moreover, the ideal gold nanoparticles suitable for the PTT should have a large absorption cross-section in the near-infrared (NIR) region. The

absorption cross-section is an important factor to evaluate the laser-induced thermal effect.¹² The reason to choose the particles' absorption at the NIR region is that normal tissues absorb and scatter light minimal at this region.¹³⁻¹⁶ However, the wavelength range between 650 and 950 nm called the first NIR window is not the optimal because of the background noise caused by the tissue auto-fluorescence and the limitation of the tissue penetration depth between 1 and 2 cm.¹⁷ A recent study showed that at the wavelength between 1000 and 1350 nm called the second NIR window light penetration depth through the tissue reaches the maximum.¹⁸ This is highly favourable for the treatment of deeply embedded tumors.

Many researches have focused on tuning the optical properties of the nanoparticles to the first NIR window for PTT application. Various gold nanoparticles like nanorods,¹⁹⁻²³ nanoshells²⁴⁻²⁸ and nanocages^{11, 29-31} have exhibited good photothermal therapeutic effects in the *in vivo* and *in vitro* experiments. The optical absorption of gold nanorods, nanoshells and nanocages are easily tuned to the first NIR window by controlling their dimensional aspect ratios (length/width or particle size/shell thickness).^{8,32} However, the nanorods seem to be the most extensively investigated particle candidate for PTT due to a few reasons. Theoretical and experimental studies have both shown that nanorods have a larger absorption cross-section than nanoshells when normalizing for particle size differences, as well as six times greater heat generation per weight of gold than nanoshells.²³ In addition, the synthetic procedure of nanorods is relatively facile

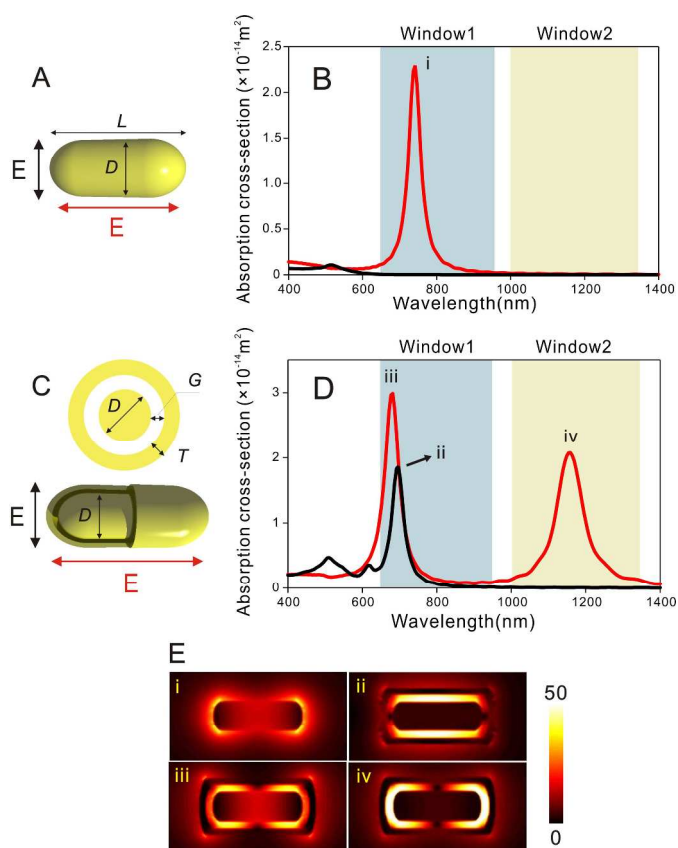


Figure 1. (A, C) Schematic illustration and (B, D) calculated absorption spectra of (A, B) a Au nanorod ($D = 20$ nm, $L = 60$ nm) or (C, D) a Au rod-in-shell particle ($D = 20$ nm, $L = 60$ nm, $T = 4$ nm, $G = 5$ nm) when illuminated by the (black) transversely or (red) longitudinally polarized light. The blue and yellow shaded areas indicate the first and second biological window (window 1 and window 2), respectively. (E) Near-field intensity distribution of the resonance mode (i) – (iv).

and their shape is easier to be controlled compared with the other two nanoparticles.³³ Furthermore, nanorods contribute to longer blood circulation time for better aggregation in the tumor cells, although their optical absorption is orientation-dependent.²³

On the other hand, there are few studies referring to the gold nanoparticles that can be employed in PTT in the second NIR window. Recently a new type of plasmonic rod-in-shell (RIS) nanoparticles via the galvanic reaction of Au-Ag rod-shells has been reported by Tsai and his co-workers.³⁴ These nanoparticles have a size smaller than 100 nm and can be tailored to be responsive in both the first and second NIR window. *In vitro* and *in vivo* experiments have clearly displayed high efficacy in NIR photothermal destruction of cancer cells, which has made the RIS structure a promising hyperthermia agent in two NIR windows. Additionally, RIS particles exhibit a more effective anticancer efficacy in the laser ablation of solid tumors compared to gold nanorods in the first NIR window with the use of an 808 nm diode laser. However, before the further development of these particles for the PTT applications a number of questions relevant to their optical properties have to be answered. For example, what is the tunable range of the optical resonances for the RIS particles? Do they have a larger absorption cross-section than the traditional gold nanoparticles such as nanorods? Are their

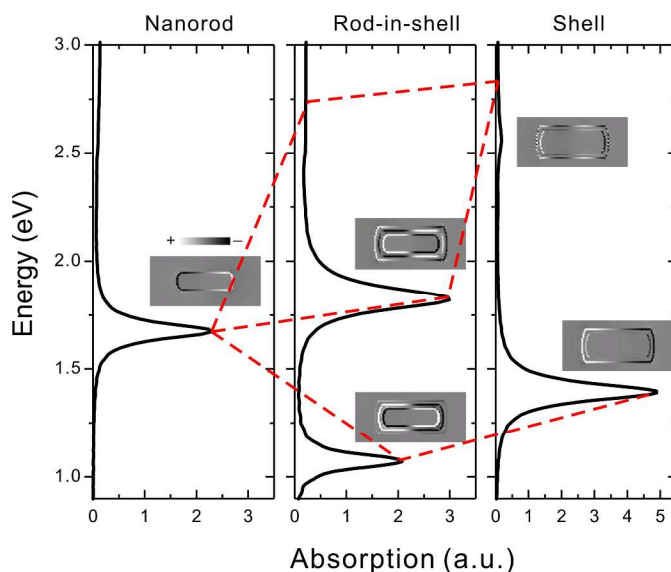


Figure 2. Longitudinal plasmon hybridization diagram for a Au rod-in-shell particle ($D = 20$ nm, $L = 60$ nm, $T = 4$ nm, $G = 5$ nm) from the individual nanorod and shell structures obtained using the FDTD simulations of their absorption cross-section.

resonances orientation-sensitive to the incident light? What is the plasmon mode for each individual resonance peak?

In this article, we theoretically investigated the optical absorption properties of the RIS particles in a systematic manner to optimize the structural dimension in terms of the absorption cross-section and the resonance wavelength. We have found that the longitudinal and transverse plasmon resonances of the RIS particles are highly tunable through both the first and the second NIR windows by controlling their core size, gap size, and shell thickness. We also compared the absorption cross-section of the longitudinal and transverse modes of a RIS particle with that of a nanorod with a similar size of the RIS's core. Consequently, we observed some merits of the RIS particles for better PTT efficacy in terms of the resonance wavelength position and tunability, absorption cross-section, and light polarization dependency.

Results and discussion

Our simulations were performed by employing a finite difference time domain (FDTD) method using the program of FDTD Solutions (Lumerical Solutions, Inc.). It is a simulation program using the FDTD method to solve the electromagnetic Maxwell equations, capable of analysing the interaction of light with complicated structures. We have used Lumerical's multi-coefficient model (MCM) to fit the empirical dielectric functions of Au and Ag^{35, 36} (see Figure.S1 in the Supporting Information). The simulation mesh size is set as 1 nm and the calculated wavelength range is from 400 to 1400 nm. The background medium of the particles is water. Figure 1A and C show the schematic illustration of a gold nanorod and a rod-in-shell (RIS) particle used in the simulation. The nanorod consists of a cylinder and two rounded ends with a diameter (D) and a total length (L), denoted as (D, L). The RIS particle has a gold nanorod core (with a diameter D and a total length L), an outer shell (with a thickness T) and a hollow gap (with a gap size G) in between, denoted as (D, L, T, G). Incident light illuminates the nanoparticle with a polarization along the transverse (black in Figure 1A, C) or the longitudinal (red in Figure 1A, C) axis

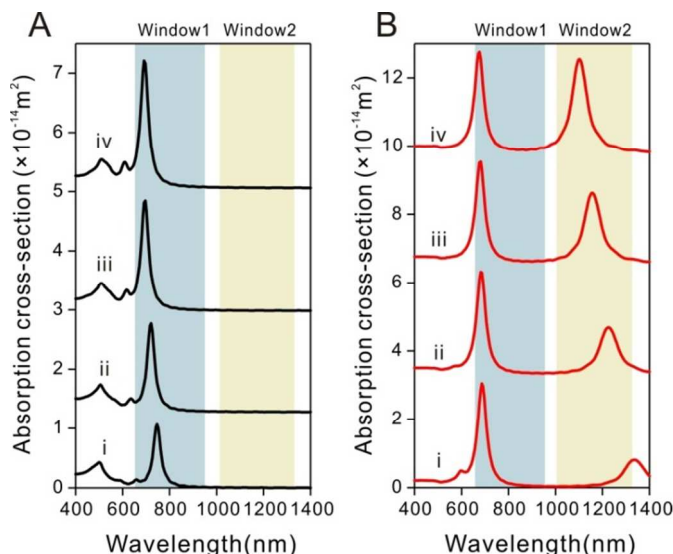


Figure 3. Calculated absorption spectra of a Au rod-in-shell particle ($D = 20$ nm, $L = 60$ nm, and $T = 4$ nm) with different gap sizes (G): (i) 3, (ii) 4, (iii) 5 and (iv) 6 nm, excited by (A) the transversely and (B) longitudinally polarized light.

of the particle. The core of the RIS particle is composed of Au and the outer shell is made of Au/Ag composite with a 1:1 ratio in order to be consistent with the average atomic ratio of Au/Ag in the energy-dispersive X-ray analysis of the experimental samples.³⁴ We have realized that the experimentally obtained RIS particles may have the irregular shape and porous shells. For the sake of simplicity, we take a simulation model with a complete and smooth shell, a regular rod-like shape and a gap filled with air. The inclusion of peanut shape and tiny holes on the shells will lead to small shifts of longitudinal and transverse modes and slight change of intensities of resonance peaks (data not shown).

Figure 1B displays the calculated absorption spectra of a nanorod with a 20 nm diameter (D) and a 60 nm length (L). Under the illumination of longitudinally polarized light, the nanorod shows a strong plasmon resonance at 742 nm locating in the first NIR window (red curve, mode **i** in Figure 1B). The corresponding on-resonance near-field intensity distribution (**i** in Figure 1E) clearly indicates its dipolar mode feature. In contrast, only a very weak resonance mode at 515 nm can be observed for the light polarized along the transverse axis (black curve in Figure 1B). To fully understand the tunability of the optical resonances, we have calculated the absorption spectra of a nanorod with different lengths from 60 to 120 nm in Figure S2 (in the Supporting Information). It is shown that as L increases from 60 to 120 nm, namely, the aspect ratio (length versus width) from 3 to 6, the longitudinal mode is shifted from the first NIR window (e.g. 742 nm for **i** in Figure S2) to the second NIR window (e.g. 1038 nm for **iv** in Figure S2) with an increment of the absorption cross-section as well. While the transverse mode remains constantly in the visible range (i.e. ~ 510 nm) with a cross-section of one order of magnitude smaller for various L . This means if we want to tailor the absorption of nanorods to the second NIR window, the size of the nanorods are most likely larger than 100 nm, which would shorten the half-life during the circulation. Moreover, the chemical synthesis of nanorods with an aspect ratio larger than 6 is still quite challenging.

For a comparison, the absorption spectra of a RIS nanoparticle (20, 60, 4, 5) with a core of the same sized nanorod (20,

60) discussed in Figure 1B are shown in Figure 1D, indicating remarkably different resonant behaviours compared to the conventional nanorods. Typically, the absorption cross-section of a RIS particle dominates the contribution to the whole extinction spectrum (see Figure S3 in the Supporting Information). Under the longitudinal excitation, the RIS particle shows two strong resonance modes at 681 (mode **iii**) and 1158 nm (mode **iv**), locating at the first and second NIR window, respectively (red curve in Figure 1D). More interestingly, a strong resonance mode at 696 nm (mode **ii**) in the first NIR window can be observed as well under the transverse polarization (black curve in Figure 1D). By careful comparison, we have found that the RIS particles have many optical advantages over the nanorods. First, the longitudinal absorption response of the RIS particle is strongly active both in the first and second NIR window and it does not require a larger dimensional aspect ratio. This means that the RIS particles with a suitable size (< 100 nm) can be easily tuned to be responsible in the second NIR window potentially with better performance for PTT applications. Next, the longitudinal absorption cross-section of the RIS particles is greater than that of the nanorod in both NIR windows even by normalizing the gold mass (see Figure S4 in the Supporting Information), which potentially indicates a better PTT efficacy. Additionally, the transverse absorption response of the RIS particles is also quite strong in the first NIR window, implying that the RIS particles can generate heat efficiently as well when the incident light polarization is along the transverse axis. More importantly, the RIS particles may be used as a type of orientation insensitive agent for the PTT application. Typically, the nanorods are randomly distributed when chemically attached to the tumors. Some of nanorods cannot work as the effective heat generation agent when the NIR laser is polarized along the short axis of the nanorods. In contrast, thanks for the overlapping of the strong transverse mode and the longitudinal mode (see mode **ii** and **iii** in Figure 1D), the RIS may always provide high PTT efficacy in the first NIR window no matter how the particles are oriented if a 690 nm laser is used. In order to gain more insights into the plasmonic properties of the resonance modes (**ii** – **iv**) of the RIS particles in Figure 1D, we also plotted their near-field intensity distribution. It can be seen from Figure 1E that the near-field intensity is in general strongly enhanced in the gap for all resonance modes (**ii** – **iv**) compared to the mode **i** in the conventional nanorods due to the plasmon coupling between core and shell.³⁷⁻⁴⁰ For the transverse mode (**ii**), the enhanced near-field regions are mainly in the gaps along the width axis with a maximum value ($|E|$) of 53, while for the longitudinal modes (**iii** and **iv**), the enhanced regions are in the gap along the length axis with a maximum value of 49 and 73, respectively. In fact, by controlling the galvanic reaction the shell of RIS particles may become porous in the Au/Ag layer,⁴¹ which allows the molecules to access the gap regions. Therefore, the enhanced near-fields in the gap of the RIS particles indicate a promising application in surface enhanced Raman scattering.⁴² The gap region filled with solvent will induce a dramatic redshift of plasmon modes due to the increased refractive index in the gap (see Figure S5 in the Supporting Information).

To understand the difference of absorption spectra between the nanorod and the RIS particle, we utilize the plasmon hybridization theory to explain their optical behaviours.³⁹ In the framework of the plasmon hybridization model, the optical spectrum of a RIS particle can be considered as the hybridization of individual nanorod and shell plasmons. The left and right panels in Figure 2 show the absorption spectra of

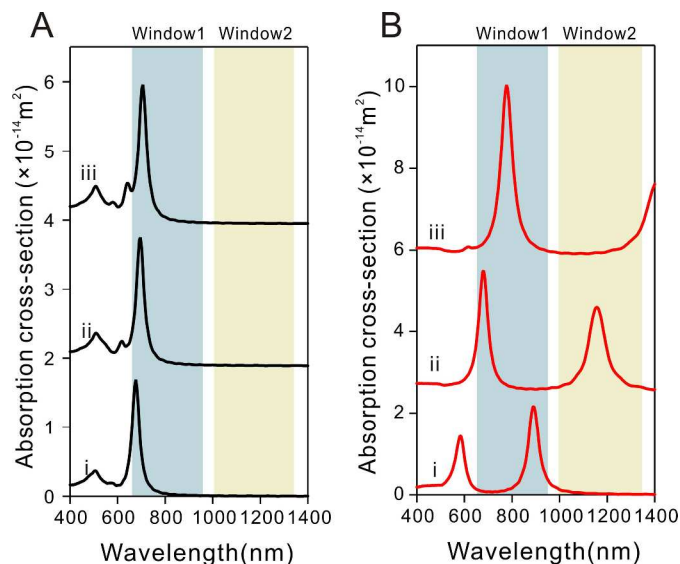


Figure 4. Calculated absorption spectra of a Au rod-in-shell particle ($D = 20$ nm, $G = 5$ nm, and $T = 4$ nm) with different lengths (L): (i) 40, (ii) 60, and (iii) 80 nm, excited by (A) the transversely and (B) longitudinally polarized light.

the individual nanorod and shell, with a dipolar rod mode and a dipolar bonding shell mode clearly visible. Then dipolar bonding shell mode is confirmed by the symmetric combination of the surface charges on the inner and outer shell (see the calculated modal surface charge distributions in the inset for the symmetries of the modes). The dipolar antibonding shell mode is expected to locate at the high-energy region and display very weak intensity due to the weak coupling to the incident light and the damping effect of interband transition. The weak mode at around 2.6 eV for the shell structure is a high-ordered bonding mode instead of the antibonding dipolar mode, confirmed by the surface charge profile. The central panel shows the absorption spectrum of the combined structure of a RIS particle with two modes via the hybridization of individual nanorod and shell dipolar plasmons. The hybridized mode at around 1.1 eV is mainly a bonding combination of the bonding shell dipole and the rod dipole, resulting in the mode shifting to a lower energy range. We refer to this mode as the RBS mode. The opposite surface charges on the nanorod and inner shell surface also explains the strong electromagnetic field enhancement in the gap region. In contrast, the surface charge calculations indicate that the mode at around 1.8 eV (referred to as the RAS mode) is mainly dominated by a bonding combination of the antibonding shell dipole and the rod dipole. We did not observe the plasmon hybridization of the high-ordered mode (e.g. the mode at 2.6 eV) with the rod dipole, because they do not have a same angular momentum in the symmetric structure. However, in some broken-symmetric structures, e.g. nanoeggs and semishells, the reduction in symmetry can relaxes the selection rules, allowing for an admixture of dipolar components in all plasmon modes.⁴³⁻⁴⁵ The antibonding combination mode of the bonding shell dipole and rod dipole does not exist is due to the small gap size induced mode conversion in the RIS particle, which has also been reported in a multilayer nanoshell system very recently.⁴⁶

To study the optical tunability of the RIS nanoparticles, we have tuned their dimensional parameters including the gap size, particle length and shell thickness and then compared the variation of their absorption spectra. Figure 3 shows the absorption spectral results of a RIS particle ($D = 20$ nm, $L = 60$

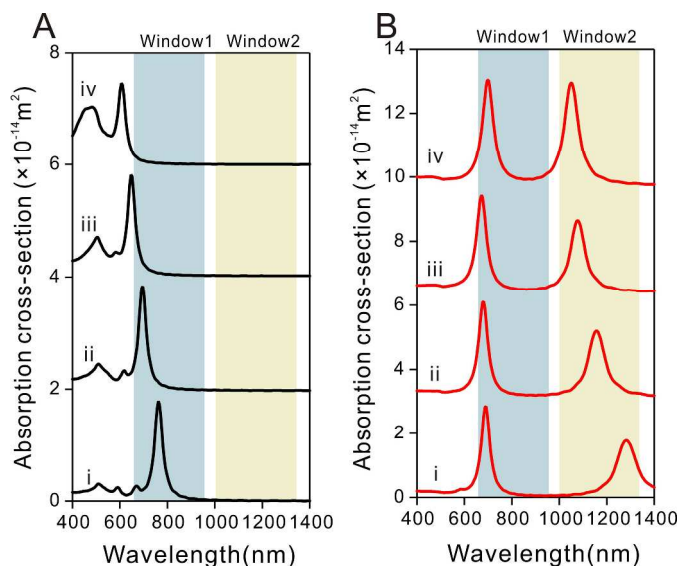


Figure 5. Calculated absorption spectra of a Au rod-in-shell particle ($D = 20$ nm, $L = 60$ nm, and $G = 5$ nm) with different shell thicknesses (T): (i) 3, (ii) 4, (iii) 5 and (iv) 6 nm, excited by (A) the transversely and (B) longitudinally polarized light.

nm, $T = 4$ nm) under two polarization directions when changing the gap size. As the gap size increases from 3 to 6 nm, the transverse mode blue-shifts from 747 to 691 nm with a gradual increment of absorption cross-section (see Figure 3A). This can be explained by the fact that the plasmon coupling between core and shell becomes weaker when the gap size increases. Conversely, the longitudinal modes exhibit a different dependence on the gap size variation. Figure 3B displays that when the gap size increases from 3 to 6 nm, the RAS mode is slightly blue-shifting from 687 to 675 nm with a nearly constant intensity, the RBS mode shows an obvious blue-shift from 1334 to 1100 nm and three times increment of intensity, indicating a much higher tunability in terms of the mode wavelength and intensity compared to the transverse mode and the RAS mode.

Figure 4 shows the absorption spectra of a Au RIS particle ($D = 20$ nm, $G = 5$ nm, $T = 4$ nm) with different lengths excited by the transversely and longitudinally polarized light. When the length (L) of the RIS particle increases from 40 to 80 nm, the transverse and longitudinal mode behave dramatically differently. The transverse mode shows a slight spectral red-shift from 676 to 706 nm and intensity increment, while the longitudinal RAS and RBS mode exhibit a red-shift of more than 190 and 500 nm (from 580 to 776 nm and from 892 nm to more than 1400 nm), respectively, indicating a much larger tunability. We expect that the RBS mode can be further tuned to be at a higher wavelength, e.g., the mid-IR range, for the application of surface enhanced infrared absorption spectroscopy (SEIRA) due to its high field enhancement. Now we switch to the discussion about the optical influence by varying the shell thickness of the RIS particle. As indicated in Figure 5, when the shell thickness is increased from 3 to 6 nm, the transverse mode and the RBS mode show a blue-shift and the RAS mode almost stay constant in terms of the wavelength and the intensity, which is very similar to the results of tuning the gap size shown in Figure 3. The blue-shift of the transverse mode and the RBS mode is mainly induced by the blue-shift of the bonding mode of the shell dipole due to the thicker shell thickness, which has little impact on the RAS mode. In the synthesis process the particle inhomogeneity and irregular

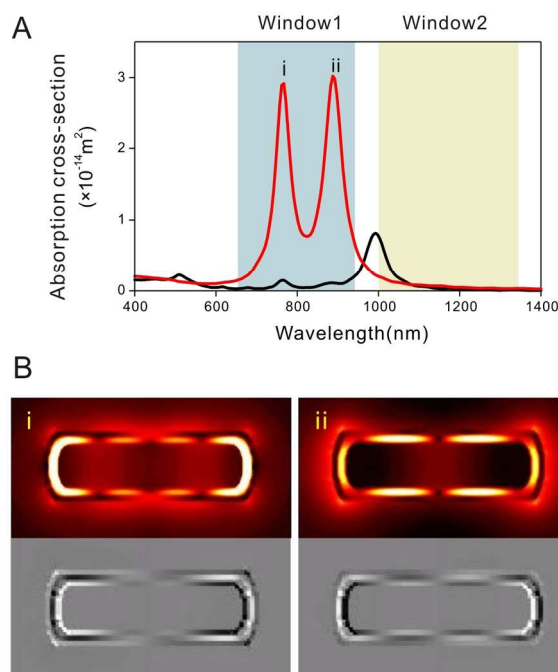


Figure 6. (A) Calculated absorption spectra of a Au rod-in-shell particle ($D = 20$ nm, $L = 80$ nm, $T = 2$ nm and $G = 3$ nm) illuminated by (black) the transversely or (red) longitudinally polarized light. (B) The corresponding (top) near-field intensity distribution and (bottom) surface charge distribution of the resonance mode (i) and (ii).

shape is inevitable. That will lead to the experimental spectra broader than our simulation result.

Comparing the spectral variation by the altering the dimensional parameters of RIS particles including the gap size, core length and shell thickness, we have found that the core length is the most sensitive parameter to impact on the optical absorption spectrum, which is similar in conventional nanorod particles. We also point out that the RBS mode has a largest optical tunability from the first NIR window throughout the second NIR window. However, the RAS mode and the transverse mode can only be possibly tailored in the first NIR window. This effect is most likely due to the stronger mode hybridization in the RBS mode, which can also be demonstrated by the large field enhancement in Figure 1 E.

In addition to the tunability of the resonance wavelength and the corresponding absorption cross-section, we note that the peak separation (i.e. the wavelength difference) between the RAS and RBS mode is highly tailorable. For instance, for the RIS particle of (i-iv) in Figure 3B, the peak separation is possibly tuned from 430 to 650 nm by changing the gap size. The high tunability and flexibility of the RAS and RBS mode position (including their high electromagnetic field enhancement) and peak separation offer a number of merits for the NIR SERS application. First, we can possibly align the RAS and RBS mode to the laser line and the Stokes Raman band to maximize the Raman signal amplification as a double-resonance substrate in NIR SERS measurement,⁴⁷ where the Raman scattering wavelength and the excitation wavelength can be separated by over 100 nm. For example, Figure 6 shows that a RIS particle (20, 80, 2, 3) has a field-enhanced double-resonance of the mode i and ii at around 780 and 890 nm, corresponding to the high-ordered RAS and RBS mode

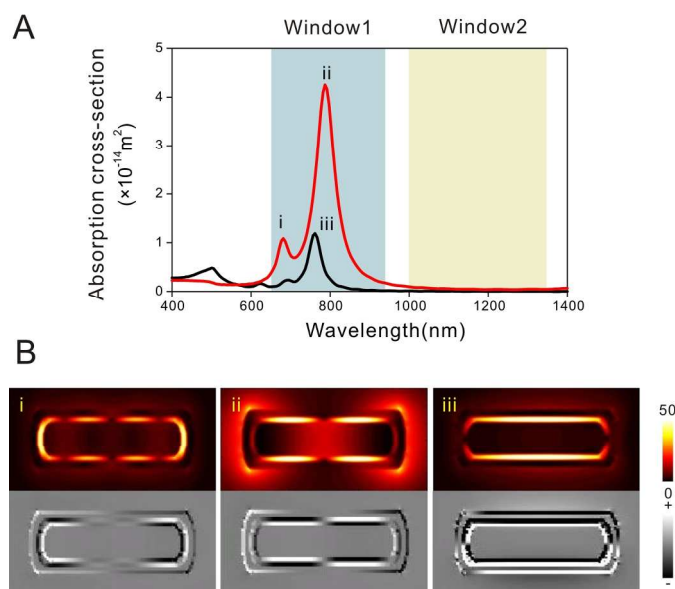


Figure 7. (A) Calculated absorption spectra of a Au rod-in-shell particle ($D = 20$ nm, $L = 80$ nm, $T = 4$ nm, and $G = 3$ nm) illuminated by (black) the transversely or (red) longitudinally polarized light. (B) The corresponding (top) near-field intensity distribution and (bottom) surface charge distribution of the resonance mode (i) – (iii).

(illustrated by the surface charge distribution in Figure 6B), respectively. For a SERS measurement of 4-aminothiophenol molecules, the mode i can be aligned to the excitation laser of 785 nm and consequently the mode ii can result in a maximal enhancement factor of the $\nu(\text{CC})$ Raman band at 896 nm (i.e. 1589 cm^{-1}). In addition, the large peak separation also allows to amplify the Raman band at a longer wavenumber, for example, $\nu(\text{=CH})$ at around 3000 cm^{-1} . Figure 7A shows another example of an orientation-insensitive RIS particle (20, 80, 4, 3) for the PTT application due to the overlapping to the mode ii and mode iii at around 800 nm. The mode ii and mode iii corresponds to the longitudinal high-ordered RBS mode and the transverse mode (confirmed by the near-field enhancement and the surface charge distribution profile in Figure 7B), respectively. Moreover, the mode ii may improve the PTT efficacy due to its large absorption cross-section.

Conclusions

We have theoretically simulated the optical absorption spectra of the gold RIS nanoparticle and optimized it through tuning the dimensional parameters including core length, gap size and shell thickness for the PTT application in the first and second NIR window. The optical resonance behaviours of the RIS particle can be explained by the plasmon hybridization theory via the hybridization of individual nanorod and shell plasmons. Gold RIS nanoparticles have a number of advantageous optical features for the PTT application compared to the gold nanorods, for example, a stronger and highly tunable optical absorption in the second NIR window with a suitable particle size (< 100 nm), a larger absorption cross-section both in the first (for the transverse mode) and second NIR window (for the longitudinal mode) for a similar particle size, and particles' orientation-insensitive light absorption due to the overlapping of the strong longitudinal and transverse mode in the first NIR window. The strong near-field enhancement in the RIS particles' gap and the

flexible tunability of the peak separation in the double-resonance mode imply the potential for the NIR SERS application as well. Therefore, the results obtained in this work will pave the way to the design and development of better plasmonic nanostructures for the PTT application in the first and second NIR window.

Acknowledgements

We gratefully acknowledge the National Natural Science Foundation of China (No. 21375087), the Natural Science Foundation of Shanghai (No.13ZR1422100) and SJTU funding (YG2012ZD03) for their financial support.

Notes and References

* Shanghai Engineering Research Center of Medical Device and Technology at Med-X, School of Biomedical Engineering, Shanghai Jiao Tong University, 1954 Huashan Road, Shanghai, 200030, China. E-mail: (H.X.) xuhong@sjtu.edu.cn; (J.Y.) yejian78@sjtu.edu.cn.

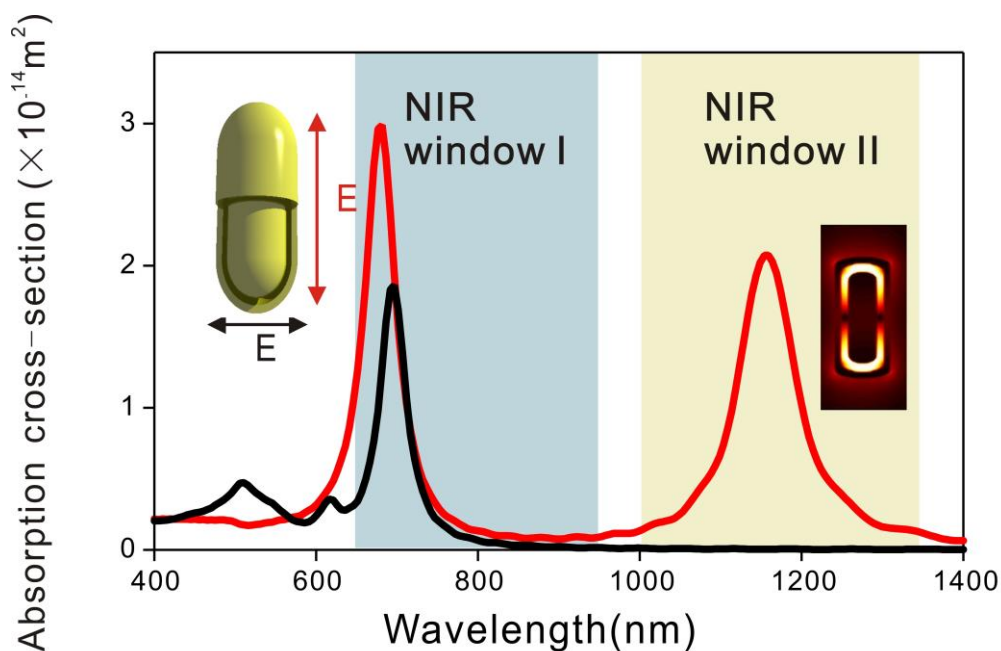
- X. Huang and M. A. El-Sayed, *Alexandria Journal of Medicine*, 2011, 47, 1-9.
- P. K. Jain, X. Huang, I. H. El-Sayed and M. A. El-Sayed, *Plasmonics*, 2007, 2, 107-118.
- L. C. Kennedy, L. R. Bickford, N. A. Lewinski, A. J. Coughlin, Y. Hu, E. S. Day, J. L. West and R. A. Drezek, *Small*, 2011, 7, 169-183.
- C. M. Cobley, J. Chen, E. C. Cho, L. V. Wang and Y. Xia, *Chemical Society Reviews*, 2011, 40, 44-56.
- X. Huang, P. K. Jain, I. H. El-Sayed and M. A. El-Sayed, *Lasers in medical science*, 2008, 23, 217-228.
- E. C. Dreaden, A. M. Alkilany, X. Huang, C. J. Murphy and M. A. El-Sayed, *ChemInform*, 2012, 43.
- M. Hu, J. Chen, Z.-Y. Li, L. Au, G. V. Hartland, X. Li, M. Marquez and Y. Xia, *Chemical Society Reviews*, 2006, 35, 1084-1094.
- X. Huang and M. A. El-Sayed, *Journal of Advanced Research*, 2010, 1, 13-28.
- X. Huang, P. K. Jain, I. H. El-Sayed and M. A. El-Sayed, *Nanomedicine*, 2007, 2, 681-693.
- E. C. Dreaden, M. A. Mackey, X. Huang, B. Kang and M. A. El-Sayed, *Chemical Society Reviews*, 2011, 40, 3391-3404.
- Y. Wang, K. C. Black, H. Luehmann, W. Li, Y. Zhang, X. Cai, D. Wan, S.-Y. Liu, M. Li and P. Kim, *ACS nano*, 2013, 7, 2068-2077.
- B. Khlebtsov, V. Zharov, A. Melnikov, V. Tuchin and N. Khlebtsov, *Nanotechnology*, 2006, 17, 5167.
- G. Hong, J. T. Robinson, Y. Zhang, S. Diao, A. L. Antaris, Q. Wang and H. Dai, *Angewandte Chemie*, 2012, 124, 9956-9959.
- H. K. Moon, S. H. Lee and H. C. Choi, *ACS nano*, 2009, 3, 3707-3713.
- D. P. O'Neal, L. R. Hirsch, N. J. Halas, J. D. Payne and J. L. West, *Cancer letters*, 2004, 209, 171-176.
- E. Yasun, H. Kang, H. Erdal, S. Cansiz, I. Ocoy, Y.-F. Huang and W. Tan, *Interface Focus*, 2013, 3.
- A. M. Smith, M. C. Mancini and S. Nie, *Nature nanotechnology*, 2009, 4, 710-711.
- K. Welsher, S. P. Sherlock and H. Dai, *Proceedings of the National Academy of Sciences*, 2011, 108, 8943-8948.
- H. Chen, L. Shao, Q. Li and J. Wang, *Chemical Society Reviews*, 2013, 42, 2679-2724.
- E. B. Dickerson, E. C. Dreaden, X. Huang, I. H. El-Sayed, H. Chu, S. Pushpanketh, J. F. McDonald and M. A. El-Sayed, *Cancer letters*, 2008, 269, 57-66.
- Y.-F. Huang, K. Sefah, S. Bamrungsap, H.-T. Chang and W. Tan, *Langmuir*, 2008, 24, 11860-11865.
- J. Perez-Juste, I. Pastoriza-Santos, L. M. Liz-Marzan and P. Mulvaney, *Coordination Chemistry Reviews*, 2005, 249, 1870-1901.
- G. von Maltzahn, J.-H. Park, A. Agrawal, N. K. Bandaru, S. K. Das, M. J. Sailor and S. N. Bhatia, *Cancer research*, 2009, 69, 3892-3900.
- J. R. Cole, N. A. Mirin, M. W. Knight, G. P. Goodrich and N. J. Halas, *The Journal of Physical Chemistry C*, 2009, 113, 12090-12094.
- A. M. Gobin, M. H. Lee, N. J. Halas, W. D. James, R. A. Drezek and J. L. West, *Nano letters*, 2007, 7, 1929-1934.
- N. Harris, M. J. Ford and M. B. Cortie, *The Journal of Physical Chemistry B*, 2006, 110, 10701-10707.
- L. R. Hirsch, R. Stafford, J. Bankson, S. Sershen, B. Rivera, R. Price, J. Hazle, N. Halas and J. West, *Proceedings of the National Academy of Sciences*, 2003, 100, 13549-13554.
- A. R. Lowery, A. M. Gobin, E. S. Day, N. J. Halas and J. L. West, *International journal of nanomedicine*, 2006, 1, 149.
- S. Kessentini and D. Barchiesi, *Session 4P8a Medical Electromagnetics, Biological Effects*, 1627.
- J. Chen, C. Glaus, R. Laforest, Q. Zhang, M. Yang, M. Gidding, M. J. Welch and Y. Xia, *Small*, 2010, 6, 811-817.
- J. Chen, D. Wang, J. Xi, L. Au, A. Siekkinen, A. Warsen, Z.-Y. Li, H. Zhang, Y. Xia and X. Li, *Nano letters*, 2007, 7, 1318-1322.
- B. N. Khlebtsov, V. A. Khanadeev, J. Ye, G. B. Sukhorukov and N. G. Khlebtsov, *Langmuir*, 2014.
- S. E. Lohse and C. J. Murphy, *Chemistry of Materials*, 2013, 25, 1250-1261.
- M. F. Tsai, S. H. G. Chang, F. Y. Cheng, V. Shanmugam, Y. S. Cheng, C. H. Su and C. S. Yeh, *ACS nano*, 2013, 7, 5330-5342.
- P. B. Johnson and R.-W. Christy, *Physical Review B*, 1972, 6, 4370.
- E. D. Palik, *Handbook of Optical Constants of Solids: Index*, Access Online via Elsevier, 1998.
- F. Hao, P. Nordlander, M. T. Burnett and S. A. Maier, *Physical Review B*, 2007, 76, 245417.
- F. Hao, P. Nordlander, Y. Sonnefraud, P. V. Dorpe and S. A. Maier, *ACS nano*, 2009, 3, 643-652.
- E. Prodan, C. Radloff, N. Halas and P. Nordlander, *Science*, 2003, 302, 419-422.
- J. Ye, L. Lagae, G. Maes and P. Van Dorpe, *Journal of Materials Chemistry*, 2011, 21, 14394-14397.
- Y. Sun and Y. Xia, *Nano letters*, 2003, 3, 1569-1572.
- D.-K. Lim, K.-S. Jeon, J.-H. Hwang, H. Kim, S. Kwon, Y. D. Suh and J.-M. Nam, *Nature nanotechnology*, 2011, 6, 452-460.
- H. Wang, Y. Wu, B. Lassiter, C. L. Nehl, J. H. Hafner, P. Nordlander and N. J. Halas, *Proceedings of the National Academy of Sciences*, 2006, 103, 10856-10860.

Journal Name

ARTICLE

44. J. Ye, L. Lagae, G. Maes, G. Borghs and P. Van Dorpe, *Optics express*, 2009, 17, 23765-23771.
45. P. Van Dorpe and J. Ye, *ACS nano*, 2011, 5, 6774-6778.
46. J. Qian, Y. Li, J. Chen, J. Xu and Q. Sun, *The Journal of Physical Chemistry C*, 2014.
47. Y. Chu, M. G. Banaee and K. B. Crozier, *ACS nano*, 2010, 4, 2804-2810.

TOC:



The plasmonic rod-in-shell nanoparticles have a number of favorable optical properties for the photothermal therapy application compared to the nanorods: increased longitudinal and transversal absorption cross-section in the NIR window I, larger and highly tunable absorption cross-section in the NIR window II, particles' orientation insensitive for the heat generation.